ELSEVIER

Chemical Physics 216 (1997) 407–415

Chemical Physics

Crystal structure and photoluminescence of single crystals of fullerene–9,9′-*trans*-bis(telluraxanthenyl) molecular complex: $C_{26}H_{18}Te_2 \cdot C_{60} \cdot CS_2$

V.V. Kveder [a], E.A. Steinman [a], B.Zh. Narymbetov [a], S.S. Khasanov [a], L.P. Rozenberg [a], R.P. Shibaeva [a], A.V. Bazhenov [a], A.V. Gorbunov [a], M.Yu. Maksimuk [a], D.V. Konarev [b], R.N. Lyubovskaya [b], Yu.A. Ossipyan [a]

[a] *Institute of Solid State Physics, Russian Academy of Sciences, 142432 Chernogolovka, Moscow district, Russia*
[b] *Institute of Chemical Physics, Russian Academy of Sciences, 142432 Chernogolovka, Moscow district, Russia*

Received 28 August 1996; in final form revised 9 January 1997

Abstract

The crystal structure of novel molecular complex of fullerene C_{60} with 9,9′-*trans*-bis(telluraxanthenyl): $C_{26}H_{18}Te_2 \cdot C_{60} \cdot CS_2$ ($BTX \cdot C_{60} \cdot CS_2$) has been investigated by X-ray structural analysis. Its photoluminescence (PL) and optical reflectivity spectra have been examined. We have found that fullerene C_{60}, donor BTX and carbon disulfide CS_2 molecules are situated at the inversion centers (1,0,1/2), (1/2,1/2,1), (1/2,1/2,1/2), respectively. The PL spectrum in C_{60} + BTX is shifted by 0.16 eV towards lower energies compared to C_{60}. The optical reflectivity spectrum of C_{60} + BTX is also different from that of C_{60}. The results are explained in terms of a decrease of the singlet exciton energy due to the strong interaction between C_{60} and BTX molecules. The decrease of PL intensity in the new complex has been found to begin at much lower temperature as compared to the pure C_{60} crystals.

1. Introduction

The crystals of fullerene C_{60} and some C_{60}-based salts and complexes can be regarded as a novel class of organic semiconductors and metals very interesting for basic research and for possible applications. The interest in such crystals has especially increased after the discovery of superconductivity in C_{60}-alkali metals salts [1], and ferromagnetism in $TDAE \cdot C_{60}$ [2] (TDAE–tetrakis(dimethylaminoethylene)). Therefore, a synthesis of new types of C_{60}-based crystals and investigation of their physical properties attracts much attention. A number of charge transfer complexes [3–6] and ion–radical salts with monoanion C_{60}^- [7–9] and dianion C_{60}^{2-} [10] were already synthesized using organic and metal organic donors.

In order to understand the electronic properties of such crystals one has to know their crystal structure. The knowledge of crystal structure is also necessary for any theoretical calculations of electronic band structure. However, the publications concerned with structural characterization of C_{60} molecular complexes are not numerous. The main reason for this is the molecular disorder caused mainly by thermally

PII S0301-0104(97)00015-3

activated rotation (or swinging) of C_{60} molecules due to their high symmetry and weak intermolecular interaction.

Here we report the results of our X-ray analysis of the crystal structure and photoluminescence measurements of single crystals of the new molecular complex $BTX \cdot C_{60} \cdot CS_2$ [11], where BTX is 9,9'-*trans*-bis(telluraxanthenyl):

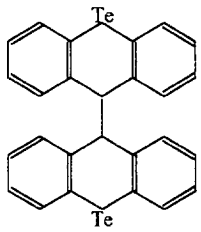

2. Measurement technique

Single crystals of the molecular complex were synthesized by evaporating a diluted equimolar solution of C_{60} and BTX in carbon disulfide CS_2 for 12 days in an argon atmosphere. The X-ray experimental data were measured at 290 K using an Enraf Nonius CAD4 diffractometer with graphite monochromated MoK_α radiation. A total of 8137 X-ray reflections were accumulated, 4037 of them were independent with $F > 4\sigma(F)$, $(\sin(\theta/\lambda)_{max} = 0.594$ Å^{-1} ($R_{av} = 0.018$ in 3908 equivalent groups). Due to the very small size of the specimen and small absorption of MoK_α radiation in this material no absorption corrections were necessary. The crystal structure was first determined by a direct method and then refined by a least-squares method in anisotropic approximation using the programs AREN [12] and SHELXL [13] with $R = 0.058$ (for all 4037 reflections). The positions of hydrogen atoms were introduced geometrically and accounted for in the calculation. The final coordinates of nonhydrogen atoms and their equivalent temperature parameters are listed in Table 1.

The photoluminescence (PL) of the $BTX \cdot C_{60} \cdot CS_2$ and C_{60} crystals was measured in the temperature range from 4.2 to 280 K using a monochromator MDR-2 and a cooled germanium detector. The overall spectral sensitivity of the experimental system was calibrated by recording the spectrum of a low-voltage tungsten lamp and dividing it by the known spectral density of the lamp emission. The experimentally measured PL spectra from the samples were then divided by the calibration spectra. So, the PL spectra reported here correspond to the number of photons (in relative units) of the given energy (i.e. dN_{ph}/dE) emitted per unit time depending on their energy E (in eV). The photoluminescence was excited by a 514.5 nm argon laser radiation or by He–Ne laser (wavelength is 632.8 nm). The laser beam was focused in a spot of about 1 mm^2 on the sample. The laser beam power was 12 mW for the Ar-laser and 2 mW for the case of He–Ne laser.

Since the crystals of the $BTX \cdot C_{60} \cdot CS_2$ were rather small (about $0.2 \times 0.2 \times 0.02$ mm^3), we measured their optical reflectivity spectra only at room temperature using an optical microscope. The measurements were made from the sample surface perpendicular to the *c*-axis of the crystal, so that the wave vector of the light was parallel to the *c* axis.

3. Experimental results

Fig. 1 represents the projection of the crystal structure along the *a* direction. The main crystal data of the complex are: $a = 10.309(1)$, $b = 10.988(3)$, $c = 12.011(1)$ Å, $\alpha = 85.20(2)$, $\beta = 71.85(1)$, $\gamma = 79.83(2)°$, $V = 1271.9$ Å^3, the space group $P\bar{1}$, $Z = 1$, the formula unit is $C_{87}H_{18}Te_2S_2$, $F(000) = 676$, $M = 1382.19$, $d_{calc} = 1.80$ g/cm^3, $\mu(MoK_\alpha) = 13.31$ cm^{-1}.

The fullerene C_{60}, donor BTX and carbon disulfide CS_2 molecules are situated at the inversion centers (1,0,1/2), (1/2,1/2,1), (1/2,1/2,1/2), respectively. The characteristic feature of the structure is the presence of C_{60} chains along the $a = 10.309$ Å, although the distance between the C_{60} centers is somewhat larger than the distance of 10.02 Å between the centers of nearest molecules in C_{60} crystals. There are no shortened $C_{60}...C_{60}$ intermolecular contacts and all the C...C distances exceed 3.60 Å (the sum of the van der Waals radii). At the same time there are slightly shortened contacts of the $BTX...C_{60}$ type: Te...C = 3.60, 3.85 and 3.84 Å and

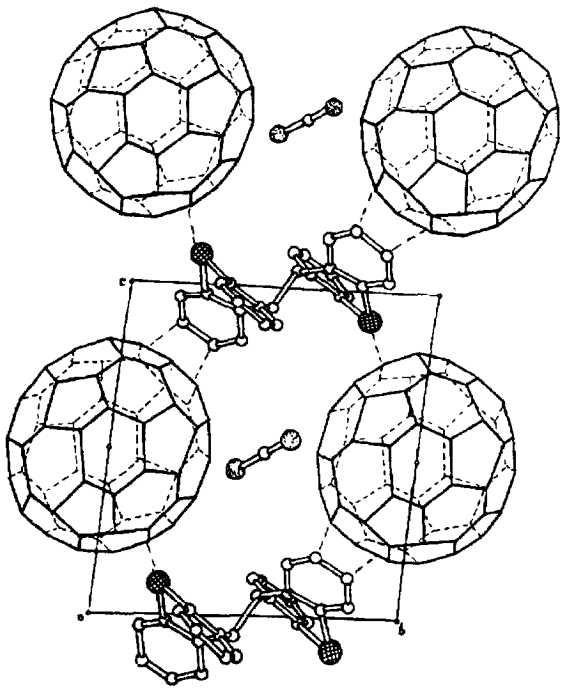

Fig. 1. Projection of the BTX·C_{60}·CS_2 structure along the *a* direction.

ten intermolecular C...C distances from 3.32 to 3.59 Å. It means that there is some overlapping of the electron wave functions of C_{60} with BTX. Some contacts between CS_2 and C_{60} are also slightly shortened compared to the sum of the van der Waals radii (S...C = 3.41 and 3.56 Å and C...C = 3.34, 3.54, 3.57 and 3.58 Å).

The accuracy in the determination of the C–C bond lengths in the C_{60} molecule itself is not high enough to estimate exactly the extent of deformation of the C_{60} molecule. This is caused by large thermal vibrations. It should be noted that though the accuracy on individual C–C bond lengths was about 0.03 Å, the actual values ranged within wider limits. Therefore, when refining the structure by the program SHELXL, we were forced to set some restrictions on the lengths of the bonds in C_{60} molecules. As a result, we obtained the same *R* factor as that calculated by the program AREN without limitations. It can be seen from Table 1 that the temperature parameters for carbon atoms in the C_{60} molecule (atoms C17–C44) are approximately 3–4 times larger than for other atoms.

Of course, the X-ray measurements at low temperature could give more precise data about the C–C bond lengths in the C_{60} molecule, but we do not see any special necessity in it because we suppose that the geometry of the C_{60} molecule is not very much affected by the intermolecular interactions in this crystal. Indeed, some small changes in the C_{60} bond lengths was noted only for anion–radical salts [9,10,14]. In this case, as the negative charge on the C_{60} molecule increases from 0 to −2, the length of the bonds tends to increase in the six-membered cycles (6:6) in the following sequence 1.355 ⇒ 1.389 ⇒ 1.399 Å and to decrease in the five-membered cycles (6:5): 1.467 ⇒ 1.449 ⇒ 1.446 Å. In our samples the EPR signal is absent and this means that the C_{60} molecules has no significant charge. This is not surprising because the comparison of the electrochemical potentials of BTX and C_{60} shows that the donor level of BTX should be by approximately 1.2–1.5 eV lower than the C_{60} LUMO level.

The BTX molecule have the conformation of a butterfly (see Fig. 2) and consists of two identical parts, connected by an ordinary C7–C7′ bond of 1.576(8) Å in length. The geometry of the BTX molecule in investigated complex is close to that in the crystal of BTX itself [15]. It is also close to that in the crystal of the charge transfer complex BTX · TCNQ [16]. The conformation of the central heterocycle ('bath') of this molecule is the following: Te and C7 atoms deviate from the plane of the remaining four atoms of the cycle in one direction by 0.63 and 0.54 Å, respectively. The planes of two benzene rings are bent back from this plane in the opposite direction by 22.8° on the average. The bending angle of the tricyclic system along the Te...C7 line equals 135.5°, that is close to the values of 138.8° and 140.5° in the BTX crystal and to 141.0° in the BTX · TCNQ crystal. The lengths of the $Te–C_{sp2}$ bonds are equal to 2.109(7) and 2.110(6) Å that is close to the mean value of 2.100(6) Å for this bond in [15], being intermediate between $Te–C_{sp}$ = 2.02(1) Å [17] and $Te–C_{sp3}$ = 2.172(3) Å [18].

Fig. 3A displays the PL spectrum of the BTX · C_{60} · CS_2 single crystal at 10 K and the result of its computer band analysis. At the energy higher than 1.1 eV, the spectrum can be reasonably good described by a sum of 12 Gaussian lines, as shown on Fig. 3A. The energy positions of the most resolved

Table 1
The coordinates of atoms and their equivalent thermal parameters U_{eq} (Å^2)

Atom	x/a	y/b	z/c	U_{eq}
Te	0.5837(0)	0.2063(0)	1.1010(0)	0.04
C1	0.4728(6)	0.2510(6)	0.9782(6)	0.03
C2	0.4026(7)	0.1626(7)	0.9556(7)	0.04
C3	0.3348(8)	0.1873(8)	0.8730(7)	0.05
C4	0.3368(8)	0.2987(8)	0.8088(7)	0.05
C5	0.4060(7)	0.3877(7)	0.8324(6)	0.04
C6	0.4746(6)	0.3650(6)	0.9176(6)	0.03
C7	0.5445(6)	0.4665(6)	0.9416(5)	0.03
C8	0.6925(6)	0.4227(6)	0.9432(5)	0.03
C9	0.7941(7)	0.4925(7)	0.8781(7)	0.04
C10	0.9296(7)	0.4584(8)	0.8828(7)	0.05
C11	0.9647(7)	0.3585(8)	0.9488(7)	0.05
C12	0.8666(7)	0.2864(7)	1.0108(6)	0.04
C13	0.7298(6)	0.3196(6)	1.0079(5)	0.03
S	0.5803(4)	−0.4195(3)	0.5423(5)	0.12
C14	0.5000(0)	−0.5000(0)	0.5000(0)	0.10
C15	0.7159(12)	0.0217(15)	0.3914(12)	0.10
C16	0.9446(16)	−0.1350(14)	0.2679(11)	0.11
C17	1.2706(16)	−.0524(19)	0.2373(13)	0.13
C18	1.0037(19)	0.3009(14)	0.3758(15)	0.12
C19	0.8364(15)	0.1987(15)	0.3215(13)	0.12
C20	0.9261(14)	−0.0011(15)	0.2333(10)	0.10
C21	1.0601(14)	0.0433(14)	0.1958(8)	0.10
C22	0.7375(16)	0.2183(17)	0.4389(16)	0.13
C23	1.0578(20)	−0.3080(13)	0.4103(17)	0.13
C24	1.2041(16)	0.1627(15)	0.2634(12)	0.11
C25	0.9126(17)	−0.2765(13)	0.4365(15)	0.12
C26	0.9645(17)	0.2369(15)	0.2894(13)	0.12
C27	1.3619(13)	−0.0785(19)	0.4034(15)	0.13
C28	1.1639(16)	−0.0639(15)	0.2024(10)	0.11
C29	0.8150(14)	0.0783(15)	0.2948(12)	0.11
C30	1.3457(12)	0.0432(18)	0.3714(14)	0.12
C31	0.7347(13)	−0.1041(14)	0.4252(13)	0.10
C32	0.7003(13)	−0.1356(15)	0.5542(14)	0.11
C33	0.8543(15)	−0.1872(15)	0.3625(13)	0.11
C34	0.6640(12)	0.1089(15)	0.4845(14)	0.11
C35	1.3204(15)	−0.1392(20)	0.3150(16)	0.14
C36	1.0932(17)	−0.1761(15)	0.2490(12)	0.12
C37	1.2646(20)	−0.2358(18)	0.3613(19)	0.15
C38	1.1537(19)	0.2542(15)	0.3560(15)	0.13
C39	1.2323(21)	−0.2764(16)	0.4819(20)	0.16
C40	1.0787(17)	0.1576(15)	0.2258(11)	0.11
C41	1.2904(15)	0.0582(17)	0.2674(12)	0.12
C42	0.8119(18)	−0.2455(15)	0.5500(17)	0.13
C43	1.1011(21)	−0.3202(14)	0.5201(18)	0.14
C44	1.1499(21)	−0.2544(16)	0.3183(16)	0.14

lines calculated from the best fit are listed in Table 2. Fig. 3B illustrate the variation of PL with temperature. The curves from 1 to 4 are the PL spectra of $BTX \cdot C_{60} \cdot CS_2$ measured at 10, 19, 31 and 50 K using 12 mW Ar-laser excitation. In Fig. 4A the PL spectrum of a pure C_{60} crystal is shown by dashed curve for comparison with the PL spectrum of the $BTX \cdot C_{60} \cdot CS_2$ that is shown by solid curve. For

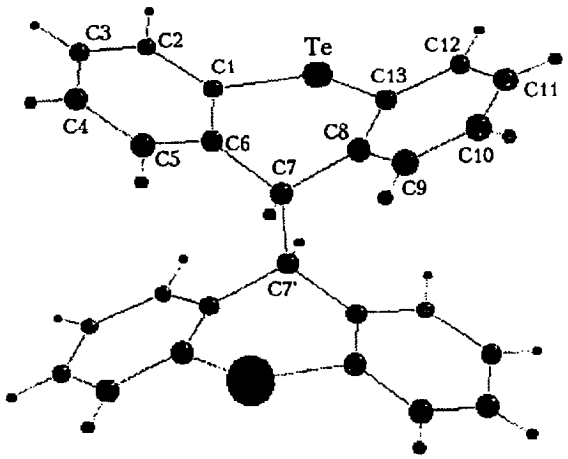

Fig. 2. Donor molecule of 9,9'-*trans*-bis(telluraxanthenyl).

convenience both spectra are normalized to their integral intensity $N_{total} = \int(dN_{ph}/dE)dE$. We have specially checked that the BTX molecules themselves as well as the CS_2 do not contribute to the luminescence in this energy range. We have also measured the PL in BTX · C_{60} crystals not containing CS_2 molecules and obtained the same PL spectra

Table 2
The energy position of some PL lines in the crystals of BTX·C_{60} ·CS_2 and C_{60} and the energy difference ΔE between them. The label (?) means that this line is not well resolved and the accuracy of energy determination is low

E_i in BTX·C_{60}·CS_2 (eV)	E_i in C_{60} (eV)	ΔE_i (eV)
–	1.665	–
1.496	1.651	0.155
1.460	1.626	0.166
1.429	1.596	0.159
1.407	(?)1.555	(?) 0.148
(?) 1.385	(?)	(?)
1.341	1.500	0.159
1.303	1.466	0.163
1.274	1.440	0.166
(?) 1.235	(?) 1.405	(?) 0.170
1.194	(?) 1.366	(?) 0.172
1.152	1.311	0.159
1.115	1.260	0.145

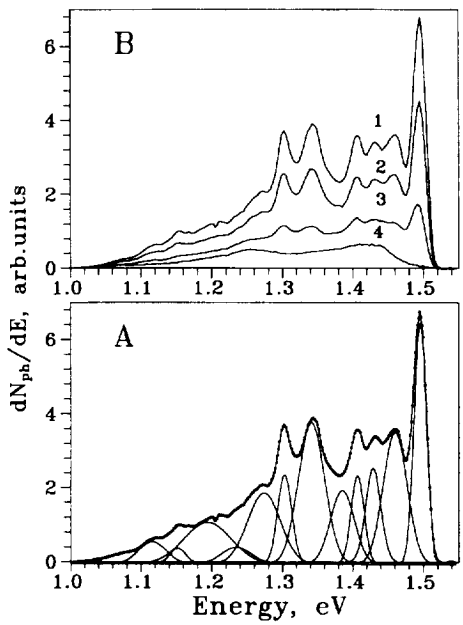

Fig. 3. PL spectra of BTX·C_{60}·CS_2 measured with 514.5 nm Ar-laser excitation. A - the PL spectrum measured at 10 K. Individual Gaussian lines are shown as it was calculated using computer fitting. B - the PL spectra measured at 10 K (1), 19 K (2) 31 K (3) and 50 K (4). The spectra correspond to the spectral density dN_{ph}/dE of emitting photons.

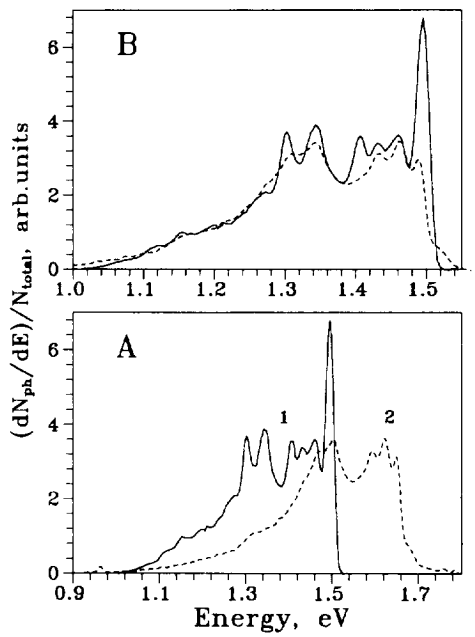

Fig. 4. PL spectrum of BTX·C_{60}·CS_2 (solid curve) and C_{60} crystal (dashed curve) measured at 10 K with 514.5 nm Ar-laser excitation. Fig. A shows original data while on Fig. B the spectrum of C_{60} crystal is shifted to the lower energy by 0.16 eV for convenience of comparison.

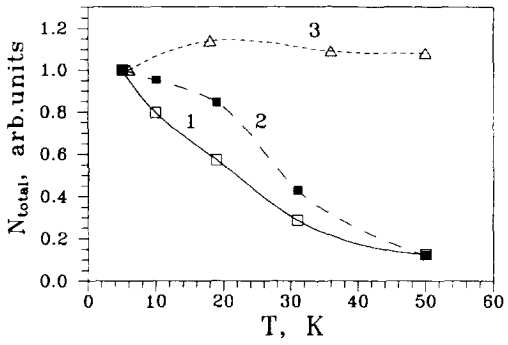

Fig. 5. PL integral intensity versus the temperature for BTX·C_{60}·CS_2 (curve 1) and C_{60} (curve 3) measured with 514.5 nm excitation (Ar-laser). Curve 2 shows the intensity of PL in BTX·C_{60}·CS_2 crystal measured using 632.8 nm excitation (He–Ne laser).

as for BTX · C_{60} · CS_2. So, the difference between the PL spectra of the complex and pure C_{60} crystal is not related to the presence of CS_2 molecules.

Fig. 5 shows the temperature dependence of the integral intensity of the photoluminescence, N_{total}, for a BTX · C_{60} · CS_2 sample (curve 1) and for a pure C_{60} sample (dashed curve 3), measured using a 514.5 nm Ar-laser excitation. In contrast to C_{60} crystals wherein the PL intensity is weakly temperature dependent at $T < 80$ K, the PL decreases rapidly starting with 5 K in the crystals of the complex. The observed decrease of the PL intensity with increasing temperature can not be explained by the change of the absorption of the laser radiation in a sample. The absorption coefficient K of the sample exceeds 10^4 cm^{-1} at the photon energy of about 2.4 eV, used for the PL excitation, while the sample thickness is about $2 \cdot 10^{-3}$ cm. Therefore, the sample absorbs all the laser light penetrating through the surface. Since the reflectivity of the sample even at room temperature is less than 20% at 2.4 eV (see Fig. 6) a possible increase of reflectivity with increasing temperature can not influence strongly the excitation rate in a sample. At least, it can not explain the decrease of PL intensity by factor 5 observed when the temperature increase from 5 to 50 K. The same is true of the C_{60} sample. The curve 2 in Fig. 5 shows the integral intensity of PL for the same BTX · C_{60} · CS_2 sample, but measured using a 632.8nm He–Ne-laser excitation instead of Ar-laser. We have found, that the quantum efficiency of luminescence for 632.8 nm excitation is approximately 6 times higher than for 514.5 nm excitation. So, the PL intensity at 2 mW He–Ne laser excitation was about the same as it was with a 12 mW Ar-laser excitation.

Curves 1 and 2 in Fig. 6 show the optical reflectivity spectra $R(E)$ measured from the *ab* plane of a sample at 300 K in polarized light. With the energy exceeding 1.7 eV the absorption coefficient K of the light in the sample is larger than 1000 cm^{-1}, and the reflection of the light from the back surface of the sample can be neglected (the sample thickness was about 20 μm). In this energy range curves 1 and 2 correspond to the directly measured reflection coefficient $R_m(E)$. In the energy range $E < 1.7$eV the absorption coefficient K is not very high and the reflection from the back surface of the sample should be taken into account. In this energy range we have measured both the reflection coefficient $R_m(E)$ and the absorption spectrum $K(E)$, and the reflectivity $R(E)$ of the sample was calculated from $R_m(E)$ and $K(E)$ using well known formula for multiple reflections. The parts of the spectra where this procedure was applied are shown in dashed line. Since the sample was rather thick (about 20 μm) we failed to

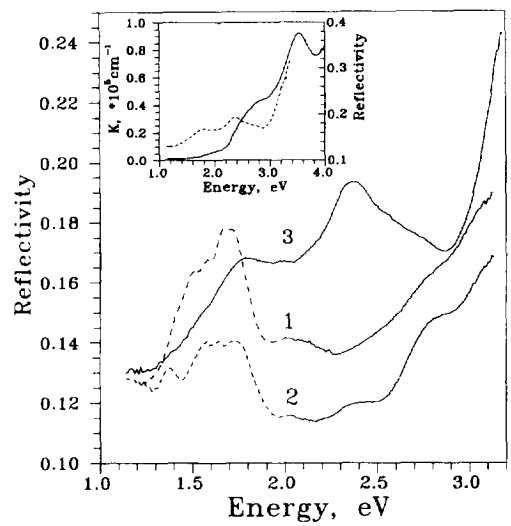

Fig. 6. Reflectivity spectra of BTX·C_{60}·CS_2 crystal (curves 1 and 2) and C_{60} crystal (curve 3) measured at 300 K. Curve 1 - the angle between light **E** vector and ***a*** vector is 30°, curve 2 is in perpendicular polarization. Insert shows the optical absorption spectrum (solid curve) and reflectivity spectrum (dashed curve) in C_{60} crystal.

measure the light absorption coefficient K at the energy higher than 2 eV. Curve 3 in Fig. 6 is the optical reflectivity spectrum of C_{60} crystal, shown for comparison.

As one can see, the reflectivity spectra of $BTX \cdot C_{60} \cdot CS_2$ differ strongly from the one of a C_{60} crystal. As contrasted from C_{60} crystals, the optical properties of $BTX \cdot C_{60} \cdot CS_2$ sample are strongly anizotropic, that is quite natural, taking into account the low symmetry of this crystal. We have found that reflection in the energy range 1.3 to 3 eV is most intensive when the light electric field is in the direction 30° deviated from the a axis in the a–b plane. Curve 1 shows the reflectivity spectrum measured in this polarization, while curve 2 is the spectrum measured in the perpendicular polarization of light. Note, that the direction of the maximal optical reflectivity corresponds to the projection of the shortest $BTX...C_{60}$ contacts on the ab plane.

4. Discussion

The electronic properties of fullerenes and fullerene based complexes are still far from clearly understood. The PL and the optical absorption of pure C_{60} crystals have been relatively well studied experimentally during the last few years (see, for example [19–26]), but there are still many open questions in the interpretation of the results. For example, it remains a question as to what extent the intermolecular interaction can break the molecular optical selection rules. It is also not clear to what extent it is possible to consider the solid C_{60} as one-electron bandlike semiconductor with h_u – derived valence band and the t_{1u} – derived conduction band. Since the allowed energy bands are rather narrow in these crystals (of the order of 0.5 eV), the Coulomb correlation and the lattice relaxation effects (as well as the lattice disorder) can make a very important contribution to their electronic properties. In the frame of one-electron bands approximation, the band gap in a C_{60} crystal is about 2.3 eV, according to the photoconductivity measurements [24]. Then the PL should be attributed to recombination of the Frenkel singlet excitons [19,20,24]. The electron–hole interaction energy is therefore very large (about 0.4 eV) and the exciton is strongly localized on a single molecule. It means that this exciton can be considered as one of excited states of C_{60} molecule in a crystal and recombination of the exciton corresponds to electronic transition from this excited state of C_{60} molecule to the ground state. A typical optical absorption spectrum that we have measured by a standard transmission technique on a crystalline C_{60} film is displayed in inset in Fig. 6 by the solid curve (the dashed curve in the inset shows the reflectivity spectrum of C_{60} crystal) This spectrum agrees well with the numerous data of the other authors (see, for example, [20–24]). As one can see, an intensive optical absorption in solid C_{60} indeed starts with the energy about 2.3 eV, but some absorption 'tail' exists starting with 1.7 eV. One can suppose that the 'tail' corresponds to the excitation of Frenkel singlet excitons. This agrees with the PL excitation spectra reported in [24].

The PL spectrum in the C_{60} (see Fig. 4A) have a complicated structure consisting of many lines, attributed in [19–22] to vibronically assistant optical transitions (false origins). Different lines in spectra correspond to the excitation of different intramolecular vibrations of C_{60} that accompany the photon emission during recombination of Frenkel exciton. For example, the authors of [22] describe the PL spectrum observed in their experiments by a superposition of 15 different false origins (see Table 1 in [22]). In some C_{60} crystals the additional lines in the PL spectra can be observed due to the presence of shallow exciton traps (X-traps) [23,26].

The interaction between molecules in C_{60}-based crystals is usually very weak compared to the interatomic interaction in the C_{60} molecule and, therefore, it can not influence strongly the vibronic frequencies of the C_{60} molecule itself. So, we can suppose that the vibronic related structure of the PL in the $BTX \cdot C_{60} \cdot CS_2$ crystal should be similar to that in the C_{60} crystal. As one can see in Fig. 4A, the PL spectrum of the $BTX \cdot C_{60} \cdot CS_2$ at 10 K is, indeed, much like the spectrum of the C_{60} crystal, but all the lines are red shifted by about 0.16 eV. To make the comparison easier, in Fig. 4B the PL spectrum of C_{60} (dashed curve) is shifted to low energy by 0.16 eV. (See also the Table 2 where the energy positions of the most resolved PL lines are listed for the $BTX \cdot C_{60} \cdot CS_2$ and C_{60} crystals). Therefore, by analogy with C_{60} crystals, we can

conclude that the PL in the BTX · C_{60} · CS_2 is mainly stipulated by the recombination of Frenkel singlet excitons associated with the C_{60} molecules, but the exciton energy is decreased by about 0.16 eV due to the interaction between the C_{60} and BTX molecules. The optical reflectivity spectra also show the shift of characteristic lines in the BTX · C_{60} · CS_2 compared to the C_{60} crystal. As one can see in Fig. 6, the reflectivity peak observed in the C_{60} at about 1.8 eV is shifted to 1.6–1.5eV in the BTX · C_{60} · CS_2. If we suppose that this reflection corresponds to the singlet exciton band, then this correlates reasonably well with the PL data. The reflection peak at about 2.3 eV in C_{60}, which is supposed to be connected with band-to-band optical transitions, is also shifted to the energy of about 2.0–2.1 eV in the BTX · C_{60} · CS_2. Note, that two additional peaks at 2.4 and 2.8 eV, existing on curve 2 in Fig. 5, were also observed in the BTX crystal. So, they probably correspond to some electronic transitions in the BTX molecules and have nothing to do with the C_{60}.

The reason for the strong (compared to the C_{60}) temperature dependence of the PL in the BTX · C_{60} · CS_2 remains unclear. The dependence of PL intensity on temperature reflect the temperature dependence of the value $W_S \cdot r_R/(r_R + r_N)$, where r_R is the rate of optical transitions from the excited state, corresponding to Frenkel singlet exciton, to the ground state, while r_N is the rate of non-radiative transitions from the same excited state (including the singlet to triplet exciton conversion). The W_S is the probability of Frenkel singlet exciton generation after absorption of photon, used for PL excitation. In case of Ar-laser excitation, the photon energy is about 2.4 eV. This energy is high enough to excite the system to electronic states, other then the electronic state responsible for photoluminescence. After photon absorption the system relaxes with the probability W_S to the Frenkel singlet exciton, but there is some probability $(1 - W_S)$ for relaxation to some other states that give no contribution to photoluminescence. For example, the intermolecular charge-transfer can be excited. In one-electron bands approximation we can say that the 2.4 eV photon excite the transitions from 'valence' band to 'conduction' band, creating 'free' holes and electrons, that can move to some electron and hole traps. Therefore, the decrease of PL intensity with increasing temperature can be associated with both, the increase of r_N and decrease of W_S. The r_N can increase, for example, due to thermally activated diffusion of excitons to the nonradiative recombination centers. The decrease of W_S can be related to thermally stimulated charge transfer processes. Note that in case of BTX · C_{60} · CS_2 crystals, the BTX molecules can be involved to charge transfer reactions. For example, the hole from the HOMO-derived level of excited C_{60} can recombine with the electron from the BTX donor level, producing BTX^+. Then the electron from C_{60}^- can jump to the empty donor level of the BTX^+ ion. It seems obvious, that the W_S should depend on the photon energy, used for PL excitation. Indeed, we have found that the PL quantum efficiency is about 6 times higher for He–Ne laser excitation, compared to Ar-laser excitation. We can suppose that this is due to the dependence of W_S on photon energy, so that the W_S for 1.96 eV excitation is 6 times larger than for 2.4 eV excitation. As one can see in Fig. 5, the temperature dependence of PL intensity for 1.96 eV excitation differs from one measured at 2.4 eV excitation. It means that the temperature dependence of W_S makes some contribution to the dependence of PL intensity on temperature, but the contribution of r_N to this dependence can not be excluded. So, the additional measurements are necessary to clarify the mechanism of temperature dependence of PL.

This work has been performed under the program 'Fullerenes and atomic clusters' of the Russian Foundation for intellectual cooperation.

References

[1] A.F. Hebard, M.J. Rosseinskii, R.C. Haddon et al., Nature 350 (1991) 600.
[2] P.-M. Allemand, K.C. Khemani, A. Koch et al., Science 253 (1991) 301.
[3] J.D. Crane, P.B. Hitchcock, H.W. Kroto et al., J. Chem. Soc. Chem. Commun. (1992) 1764.
[4] A. Izuoka, T. Tashikawa, T. Sugawara et al., J. Chem. Soc. Chem. Commun. (1992) 1472.
[5] A. Izuoka, T. Tachikawa, T. Sugawara et al., Chem. Lett. (1992) 1049.
[6] P. Wang, W-J. Lee, I. Shcherbakova et al., Synth. Metals 64 (1994) 319.
[7] A. Penicaud, A. Perez-Benitez, V.R. Gleason et al., J. Am. CHem. Soc. 115 (1993) 10392.

[8] U. Bilow and M. Jansen, J. Chem. Soc., Chem. Commun. (1994) 403.
[9] W.C. Wan, X. Liu, G.M. Sweeney and W.E. Broderick, J. Am. Chem. Soc. 117 (1995) 9580.
[10] P. Paul, Z. Xie, R. Bau et al., J. Am. Chem. Soc. 116 (1994) 4145.
[11] D.V. Konarev, R.N. Lyubovskaya, O.S. Roschupkina et al., Mendeleev Commun. (1996) 3.
[12] V.I. Andrianov, Kristallografiya (Russian) 32 (1987) 228.
[13] G.M. Sheldrick, SHELX-93, Program for Crystal Structure Determination, University of Cambridge, UK, 1993.
[14] S. Liu, Y.-J. Lu, M.M. Kappes and J.A. Ibers, Science 254 (1991) 408; H.-B.Burgi, E. Blanc, D. Schwarzenbach, S. Liu, Y.-J. Lu, M.M. Kappes, J.A. Ibers, Angew. Chem. Int. Ed. Engl. 31 (1992) 640.
[15] K.Sh. Karaev, H.G. Furmanova, N.V. Belov et al., Zhur. Strukt. Khim. (Russian) 22 (1981) 16.
[16] R.M. Lobkovskaya, R.P. Shibaeva and O.N. Eremenko, Kristallografiya (Russian) 28 (1983) 276.
[17] S. Foãst, J. Chem. Soc. B (1979) 9 414.
[18] J. Bergman and L.J. Engman, J. Organomet. Chem. B 181 (1979) 335
[19] Ying Wang, J.M. Holden, A.M. Rao, P.C. Eklund, U.D. Venkateswaran, DeLyle Eastwood, R.L. Lidberg, G. Dresselhaus and M.S. Dresselhaus, Phys. Rev. B 51(7) (1995) 4547.
[20] D. Dick, X. Wei, S. Jeglinski, R.E. Benner, Z.V. Vardeny, D. Moses, V.I. Srdanov and F. Wudl, Phys. Rev. Lett. 73 (1994) 2760.
[21] R.D. Averitt, V.O. Papanyan, J.A. Dura, P. Nordlander, N.J. Halas, Chem. Phys. Lett. 242 (1995) 592.
[22] M. Diehl, J. Degen and H.H. Schmidtke, J. Phys. Chem. 99 (1995) 10092.
[23] W. Guss, J. Feldmann, E.O. Goebel, C. Taliani, H. Mohn, W. Muller, P. Haussler and H.-U. ter Meer, Phys. Rev. Lett. 72 (1994) 2644.
[24] S. Kazaoui, R. Ross and N. Minami, Phys. Rev. B 52 (1995) R11665.
[25] G. Kato, C. Yokomizo, H. Omata, M. Sato, T. Ishii, K. Nagasaka, Solid State Commun. 93 (1995) 801.
[26] V.D. Negrii, V.V. Kveder, I.N. Kremenskaya, R.K. Nikolaev and Yu.A. Ossipyan: Proceedings of International workshop 'Fullerens and Atomic Clusters', St. Petersburg, June 19–24 (1995).